

# An Analysis of a Stochastic Urban Propagation Model Using Ray Tracing Generated Results

Carmen Cerasoli, James Dimarogonas, Chad Edwards, William Franklin  
The MITRE Corporation  
Eatontown, NJ

## ABSTRACT

*A stochastic urban electromagnetic propagation model for non-line-of-sight (NLOS) paths was critically examined by comparing model behavior to ray tracing simulations in four city environments. We focus on the quality of model/data fit and the ability to a priori set model parameters based on city geometry and building materials.*

*The stochastic model was found to fit simulated data well in typical cities. However, relating model parameters to city geometry metrics met with limited success. This is most likely due to the difficulty in characterizing city geometry, and the underlying physics of the model. The complex process of electromagnetic propagation is modeled as a simple one-dimensional random walk, leading to diffusion-like behavior. The model does possess utility in its ability to provide easily computed estimates of urban propagation path losses and is an improvement over other empirical models.*

## I. INTRODUCTION

Providing robust radio communications within an urban environment for highly mobile forces independent of a fixed infrastructure has always been a challenge for the modern Army. Not only do the propagation characteristics limit achievable ranges, they are difficult to accurately predict and possess high variability. The network designer needs to be able to quantify the ranges and associated variability and offer solutions to provide a robust, well-connected network that can support Military Operations in Urban Terrain (MOUT). The complexities of network modeling create the need for an easily implemented, physics-based urban ground-to-ground propagation model for assessing the networking capabilities and performance of proposed DoD RF communications systems. Such a propagation model would provide quick estimates of signal strengths in generic cities without using computationally intensive techniques such as ray tracing where detailed building structure data (non-generic) are required. This model would not be used to plan a specific deployment with

highly accurate predictions on a node-by-node basis, but rather provide a generic assessment of the connectivity expected for the network as a whole. This would provide estimates for the network behavior of a large number of nodes and parameter variations without being so computationally intensive as to create unreasonably long run times. A number of highly empirical models exist for elevated base stations to ground mobile users such as the Okamura-Hata or Walfisch-Ikegami models [1]. Models exist for NLOS, ground-to-ground, paths [2, 3] but are designed for relatively orderly urban building arrangements. Franceschetti and others [4, 5] have recently proposed stochastic models for electromagnetic propagation in urban environments. These models are based on a well defined physical picture where RF propagation is modeled as a one-dimensional random walk. They predict the functional form for received signal strength versus transmitter distance and require at most three parameters: an effective power, a measure of inter-building spacing and a measure of the building reflection characteristics.

This paper critically examined the capabilities of stochastic propagation model and attempted to relate city characteristics to model parameters. The analysis relied on ray tracing results generated for four cities with very different geometries: Rosslyn, Ottawa, Berne and Helsinki. Three frequencies were chosen, 400, 900 and 2100 MHz, and building material characteristics were varied. We investigated the ability to set model parameters using city geometry information. Such a capability would allow model prediction by simply computing the appropriate city geometry metric(s) and relating them to model parameters.

Section II provides a brief discussion of the ray tracing approximation and defines the simulation strategy. The stochastic urban model is described in Section III, and ray tracing simulation results are presented in Section IV. Model and simulation results are compared in Section V where we attempt to relate city geometry metrics to model parameters. Section VI discusses the models capabilities and short comings and presents two approaches for model

improvement and utilization. Section VII summarizes the work.

## II. THE RAY TRACING APPROXIMATION

Electromagnetic propagation can be determined in any environment by solving Maxwell's equations subject to appropriate boundary conditions. Unfortunately, this is not easily achieved either analytically or with numerical methods. In general, approximations must be made regarding the nature of the propagation, and ray tracing is one such approximation. The details of ray tracing can be found in numerous sources [6] and are not given here. Simply put, this method treats electromagnetic waves as rays that propagate according to the laws of geometrical optics. Those rays can undergo numerous reflections, diffractions and transmissions based on detailed information about the positions, shapes and surface characteristics of the urban structures. Snell's law gives the distribution of the scattered wave field and physical optics provides the scalar magnitudes, which are summed to produce the final result.

The ray tracing solutions were obtained using a commercial software package, *Wireless Insite* by REMCOM. The Urban Canyon or 2D approximation was used in here, where only paths connecting the Tx and Rx in the two dimensional, horizontal plane are considered and there are no diffractive paths over building. This is a reasonable assumption for ground-based antennas at 2 to 3 meters in many urban areas.

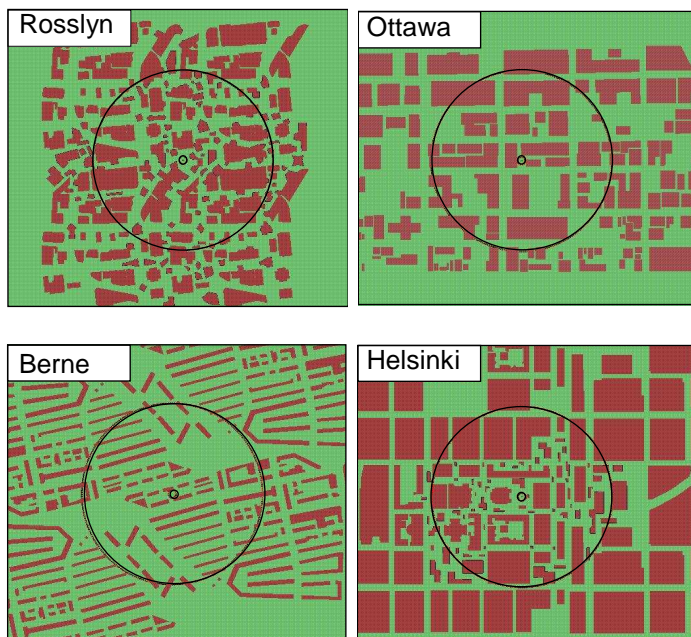


**Figure 1. Aerial view of the four cities used in this study: Rosslyn, Ottawa, Berne and Helsinki**

An aerial view of the four cities used in this study is shown in Figure 1. All have very different geometric structures and the city geometry files were available within the *Wireless Insite* software. Receiver positions greater than 200 m from the transmitter were sought and the city areas provided were smaller than required. A larger urban area was created by merging four identical cities into a single, larger urban area. This is seen most clearly for Rosslyn.

The small and large circles in Figure 1 are at radii of 10 and 230 m, respectively. A vertically polarized half wave dipole antenna at 2 m height radiating 30 dBm was placed at the circle center. Half wave dipole antennas at 2 m height were positioned on concentric circles of radii 10 to 230 m every 5 m centered on the Tx. Receiver spacing was approximately 5 m on each circle circumference, and received powers were only computed outside of the buildings.

Powers were averaged over each radius and additional averaging was done by repeating the computation with a new Tx position and set of receiver radii. The new positions were displaced from 70 to 130 m to the four cardinal compass points, resulting in data for five Tx/Rx positions, Center, North, South, East and West.

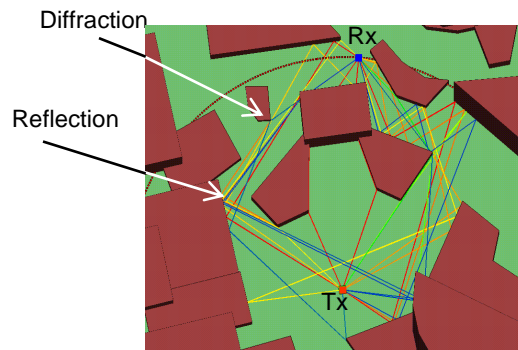


**Figure 2. Reflecting and diffracting paths connecting transmitter and receiver.**

The stochastic urban propagation model is based on the assumptions that many reflections occur between Tx and Rx. Figure 2 shows a typical example of rays connecting a Tx and Rx. Each line is a ray and the color coding goes from strongest, red, to weakest, blue. Numerous reflections and diffractions can be seen.

A valid criticism of our method is that we are treating ray tracing results as reality for comparison to an analytical model. The ray tracing approximation has been shown [6] to provide good power estimates when properly applied. It is a practical technique compared to the time consuming and costly approach of a measurement program in multiple

cities with different geometries and building materials. Our method provides insight into the stochastic model accuracy and usefulness under varying urban settings and conditions.

### III. The Stochastic Urban Propagation Model

Detailed descriptions of the stochastic urban propagation model can be found in [4, 5] and a simple description is presented here. Scattering can be categorized according to whether the scatterers are electrically large or small (scattering dimension large or small relative to the radiation wavelength,  $\lambda$ , respectively). In the former case, electromagnetic waves are modeled as rays that reflect according to Snell's law yielding reflection coefficients. In the latter case, photons are modeled as hard spheres that reflect randomly from point scatterers with an absorption coefficient,  $\gamma$ . Simplifying assumptions in [4] allow both categories to be modeled as a one-dimensional random walk. In particular, the electrically small case resembles a diffusion process with an effective mean free path ultimately determined by the dimensions and separations of the scatterers.

In general, reflection coefficients are a function of incident angle and polarization; the present ray tracing simulations used constant reflection coefficients to allow comparison with the stochastic model assumption of constant  $\gamma$ . The number of reflections between the Tx and Rx is related to an average inter-building spacing embodied in the inverse of the photon mean free path,  $\eta$ , (1/m). In the electrically small case, the following expression for the power flux density,  $S$  (watts/m<sup>2</sup>) versus distance from the transmitter,  $r$ , was derived [4]

$$S = 1/(4\pi r^2) [ (1-\gamma)\eta r \exp(-\alpha r) + \exp(-\beta r) ] P_{\text{eff}} \quad (1)$$

where

$$\alpha = \sqrt{1-(1-\gamma)^2} \eta \quad (2)$$

$$\beta = 1-(1-\gamma)^2 \eta \quad (3)$$

and  $P_{\text{eff}}$  represents an effective power. The power at a given receiver is computed as

$$P = S G_r \lambda^2 / 4\pi \quad (4)$$

where  $\lambda$  is the RF wavelength and  $G_r$  is the receiver antenna gain. The authors [4] note that the second term of Equation (1) dominates the expression for relatively small  $r$ . For realistic values of  $\eta$  and  $\gamma$  and  $r > 50\text{m}$ , Eq. (1) becomes

$$S \approx 1/(4\pi r^2) [\exp(-\beta r)] P_{\text{eff}} \quad (5)$$

$S$  depends on frequency only by allowing  $\gamma$  to be a function of frequency.  $\eta$  is solely geometry dependent and  $S$  does not explicitly depend on frequency. This explicit frequency independence of the power flux density is consistent with two assumptions of the model and appears in both Eq. (1) and (5). First, only specular reflections at building surfaces are considered while frequency dependent diffractions around building edges are not. As shown in Figure 2, diffractive paths can contribute to the received signal. Second is the assumption that the power at a receiver is obtained by “summing the intensity of all different waves reaching the receiver” [4]. This corresponds to incoherent ray addition and neglects any constructive/destructive interference effects which can occur.

### IV. RAY TRACING RESULTS

The ray tracing computations used the four city geometries shown above and three narrow band frequency waveforms at 400, 900 and 2100 MHz. Two constant reflection coefficients were used, -0.8 and -0.2, simulating good and poor reflecting surfaces, respectively. Figure 3 shows averaged power flux density,  $S$ , versus distance and the color and line codes shown for Rosslyn apply to all the results. A linear  $r$  axis was used to emphasize the approximate exponential nature of the solution, and near straight lines indicate the quality of the model fit.

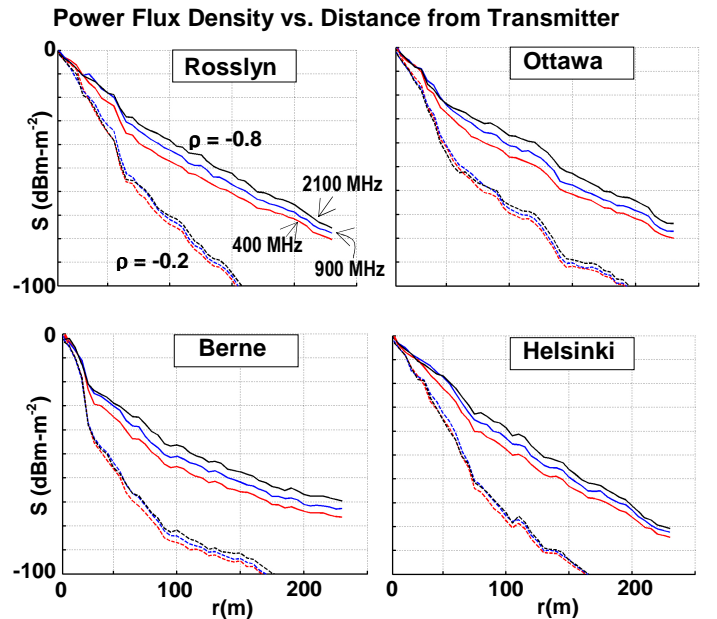


**Figure 3. Averaged power flux density versus distance for the four cities, three frequencies and two building reflection coefficients.**

Near exponential behavior past  $r \sim 50\text{m}$  exists for Rosslyn, Ottawa and Helsinki. Berne deviates from this behavior

which is probably due to the long, narrow structure of the city streets compared to the other cities. The power flux density decays rapidly for a lossy reflective surface,  $\rho = -0.2$ , as expected, and there is minor frequency dependence for this lossy surface case.

The  $\rho = -0.8$  results show frequency variation. This can be traced to the manner in which the multiple rays arriving at the receiver are summed to obtain received power and the inclusion of diffracting rays. The electric field at any receiver can be written as

$$E = \sum_{k=1}^{k=N} a_k \exp(-i\theta_k) \quad (6)$$

where  $N$  is the number of direct, reflected and diffracted rays reaching the receiver.  $a_k$  and  $\theta_k$  are the field strength amplitude and phase of the  $k^{\text{th}}$  ray, respectively. The power may be obtained *coherently* by

$$P_{\text{coherent}} = E^* E \quad (7)$$

or *incoherently* by

$$P_{\text{incoherent}} = \sum_{k=1}^{k=N} a_k^2 \quad (8)$$

Powers obtained coherently can show constructive and destructive interference effects, while powers obtained incoherently will not. Neither summation method may be appropriate in many situations. Computationally, coherent addition implies precise knowledge of all building positions (to within  $1/2$  wavelength), an unrealistic assumption. Incoherent addition negates all possible interference effects which can be at play.

*Wireless Insite* provides an alternative to these two extremes, *correlated* summation. A filter is used to determine which rays have followed a similar set of paths. Examples of the filter criteria are the time of arrival or angle of arrival/departure. The electric field is summed coherently for all these “bundled” rays and the set of bundled rays are then summed incoherently. This method allows for constructive/destructive interference effects but does not over-estimate them as would be the case for coherent addition of all rays.

The other reason for the frequency dependency is due to inclusion of diffractive paths. Diffraction around building edges is frequency dependent with higher frequency signals being attenuated more than lower frequency signals.

A series of computations were performed with reflections only and incoherent summation to ascertain the effects of

diffraction and interference. When only reflections are allowed, the incoherent summation yields no frequency dependence for the power flux density. The use of correlated summation results in frequency dependency where the 400 MHz signal suffers greater destructive interference than at 2100 MHz. Also, very little difference exists than at 2100 MHz between correlated and incoherent summation. This is to be expected as the filter criteria become more difficult to satisfy as the wavelength becomes shorter and the rays tend to de-correlate.

Allowing diffractive paths greatly increases signal strength and also increases the (on average) destructive interference at the lower frequencies. This is consistent with greater ray correlations as the wavelength increases, while the bias toward destructive interference is a result of the Rayleigh distribution for multi-path rays. The difference between the use correlated or incoherent summation and the inclusion of diffraction are minimized when  $\rho = -0.2$ . The rays lose substantial energy upon reflection and combinatory effects are small.

## V. SIMULATION RESULTS VERSUS MODEL

The simulation results can be fit to the solutions given in Eqs. (1) and (5) although a number of questions arise. The full solution, Eq. (1) is valid only for  $r$  greater than  $\sim 10\eta^{-1}$ , based on inverse Fourier Transform approximation used in [4]. This approximation translates to requiring numerous reflections (along NLOS paths) and satisfying the stochastic nature of the model. In our cities, this corresponded to  $r > 30$  m where the far field solution of Eq. (5) and Eq. (1) are nearly identical. Note that  $P_{\text{eff}}$  need not equal the true radiated power. Also, using Eq. (1) and attempting to find the best  $\eta$ 's and  $\gamma$ 's creates the following difficulty. One finds a set of best fit  $(\eta, \gamma)$  pairs with relatively small variance between data and curve fit,  $\sigma$ . These pairs satisfy Eq. (3) for a constant  $\beta$ , and the pair defined by the precise  $\sigma$  minimum may not always be meaningful. Unrealistic values of  $\eta$  and  $\gamma$  can occur where their roles are “flipped”, that is, large values of  $\eta$  combine with small values of  $\gamma$  which are inconsistent with the geometry and the known reflection coefficient.

Based on the previous discussions concerning correlated versus incoherent summations and the contribution of diffractive paths, we focus on the 2100 MHz results where both effects are at a minimum. Simulation results will be more in the spirit of the incoherent summation assumed in the stochastic model.

Figures 4 and 5 show the values of  $\beta$  and the curve fit variance,  $\sigma$ , for all four cities and two values of building reflection coefficient. Three methods were used to obtain  $\beta$ , and are labeled a, b and c. Method (a) used the averaged power at all the radial positions from  $r = 10$  to 230 m and allowed the effective power to be a free parameter. Method (b) is similar to (a) but only used radial points from 50 to 230 m. Method (c) set  $P_{\text{eff}}$  to be the true radiated power and used all the radial positions. Method (b) is the one most in the spirit of the model ( $r > 10\eta^{-1}$ ), while Method (c) minimized unknown parameters by setting  $P_{\text{eff}}$  and is preferred from a practical point of view.

The best data to model fit (lowest values of  $\sigma$ ) were always found for Method (b) as expected. Only radial points  $r > 10\eta^{-1}$  are included and  $P_{\text{eff}}$  is a free parameter. For good reflecting surfaces, the quality of the fit was good with  $\sigma$  always below 5 dB, and  $\beta$  depended weakly on the method. For poorly reflecting buildings the same is true except for Berne. Note the scale for  $\sigma$  is 3x larger for  $\rho = -0.2$ . Again, given Berne's peculiar building geometry, this is not surprising.

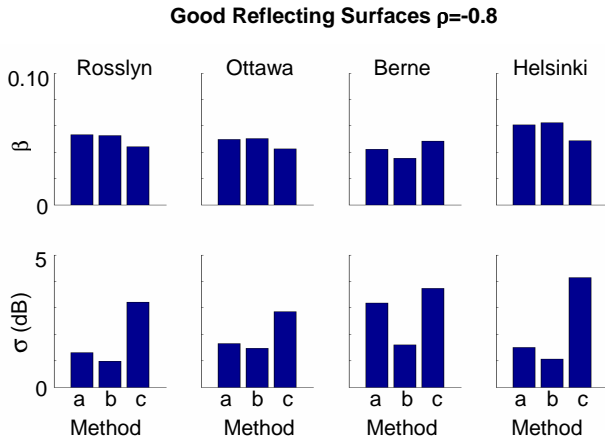


**Figure 4. Values of  $\beta$  and associated variance,  $\sigma$ , obtained by three curve fitting methods for four cities with good reflecting surfaces.**

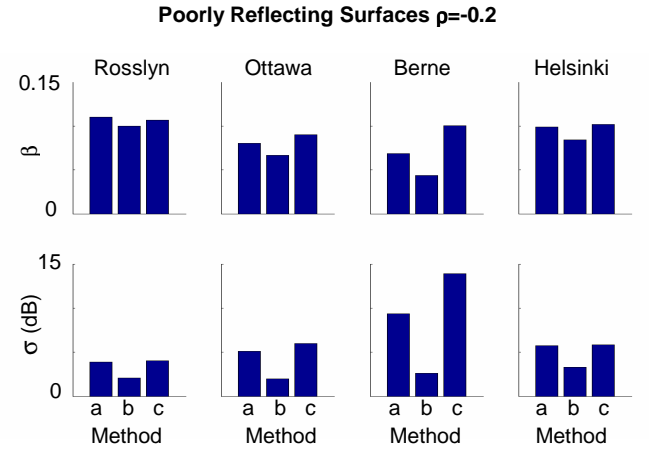


**Figure 5. Values of  $\beta$  and associated variance,  $\sigma$ , obtained by three curve fitting methods for four cities with poor reflecting surfaces.**

$\gamma$  is related to  $\rho$  as follows.  $\rho$  is the reflection coefficient for the electric field,

$$\rho = E_R/E_I \quad (9)$$

where the subscripts refer to the reflected and incident electric fields, respectively. The ratio of reflected to incident power is given by  $\rho^2$ . As  $\gamma$  describes the probability of a photon (energy/power) being lost or absorbed,  $\gamma$  and  $\rho$  are related by:

$$\gamma = 1 - \rho^2 \quad (10)$$

The two values chosen,  $\rho = -0.2$  and  $-0.8$ , yield  $\gamma = 0.96$  and  $0.36$ , respectively. The  $\gamma$ 's represent highly absorbing and relatively good reflecting surfaces, respectively.

This study sought ways in which the stochastic model can use *a priori* information on city geometry and knowledge of building surface characteristics. Average inter-building spacing is not a well-defined metric in complex urban environments, and trying to develop any such metric might not be a fruitful exercise. One simple procedure was to scan through the urban area along different orientations and accumulate statistics on the distances between structures. This is shown schematically in Figure 6. Scans along the horizontal, vertical and both diagonal directions are depicted, and statistics on all the arrow lengths are gathered. Better metrics may exist but this does provide some statistical measure of the urban environment. Histograms of these “open area distances” were used to define length scales associated with the four directions plus one based on all directions combined. A summary of these length scales is given in Table I.



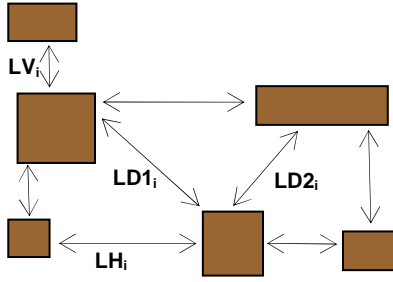


**Figure 6. Schematic representation for defining inter-building spacing.**

**Table I. Estimated Values for Inter-Building Spacing**

	Vert	Hor	Diag	Diag	Total
Rosslyn	34	29	26	25	28
Ottawa	54	41	37	37	41
Berne	50	31	26	26	31
Helsinki	28	29	21	22	25

Some correlation between these length scales and the cities shown in Figure 1 can be observed. Berne showed large disparity between horizontal and vertical scale, Rosslyn was relatively uniform, etc. One should be cautious about ascribing too great a significance to the inter-building spacing for two reasons. First it is not an easily defined metric. Second, and more importantly, it may not be the parameter controlling the problem physics. A more appropriate parameter may be the building cross sections and will be discussed in Section VI.

How well this *a priori* strategy works can be assessed by comparing  $\eta^{-1}$  to the estimated inter-building spacings given in Table I.  $\eta$  is obtained using the best fit  $\beta$  and the known value for  $\gamma$  via Eq. (3) and Eq. (10). For simplicity, we only use the values based Total histograms, and Figure 7 shows the ratio between  $\eta^{-1}$  and  $L$  for the four cities and the three curve fitting methods for determining  $\beta$ . For a “perfect” model and “perfect” estimate of inter-building spacing,  $L$ , the ratio for all points should be equal.

The data summarized in Figure 7 can be viewed optimistically by noting that the ratio of  $\eta^{-1}/L$  is approximately 2-1/2. This implies that one can view an urban area from above, estimate  $L$  as done here, make an estimate of surface reflecting based on knowledge of typical building material, compute  $\beta$  and make predictions

of average signal strength in an urban setting. The pessimistic view would be to note that the ratios vary too greatly from the mean.

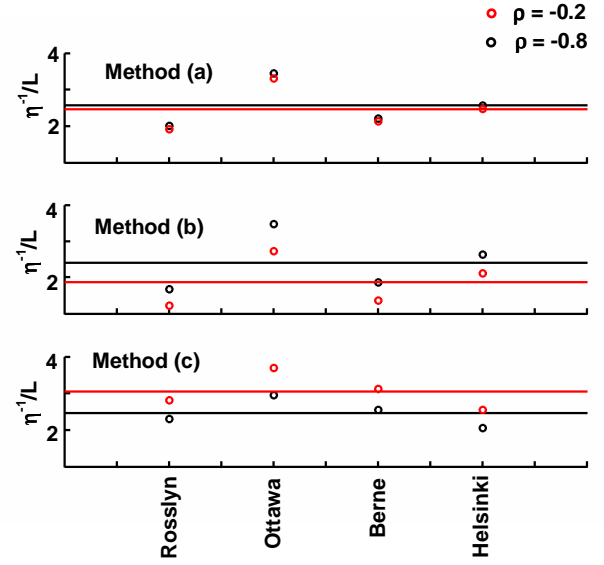


**Figure 7. The ratio of inferred inter-building spacing  $\eta^{-1}$  and  $L$  for two reflection coefficients and the four cities using three different methods to obtain  $\eta^{-1}$ . Straight lines are mean value.**

## VI. DISCUSSION

It is gratifying that relating the stochastic model parameter  $\beta$  to a crude estimate of inter-building spacing,  $L$ , meets with some success. This is the optimistic interpretation of the results in Figure 7. The difficulties in relating  $\beta$  and  $L$  (the pessimistic view) may be due to the model assumptions in a number of ways. The very complex process of electromagnetic propagation has been replaced with a leaky diffusion model, leaky in the sense that “photons” are removed based on the value of  $\gamma$ . Frequency dependent phenomena such as diffraction and coherence cannot neatly fit into this framework. Also, the mean free path,  $\eta^{-1}$ , and the inter-building spacing are equated. In reality, the mean free path for a photon (or ray) is given by the product of density of reflectors,  $n$  (number/m<sup>2</sup>) and the cross section of those reflectors,  $\sigma_{xc}(m)$ , where we are considering a two-dimensional situation.

$$\eta = n \sigma_{xc} \quad (11)$$

Only in the restrictive case of uniformly positioned square reflectors at spacing  $L$ , and reflector sizes small relative to  $L$ , can the simple relationship between mean free path,  $\eta^{-1}$ , and  $L$ , be valid where

$$\eta = L^{-1} \quad (12)$$

This simplification of equating  $\eta$  to  $L^{-1}$  may be the root difficulty in setting  $\eta$  in terms of  $L$ .

The above does not negate the stochastic model's utility. Many instances exist in engineering where complex processes are modeled as diffusive-like processes. Turbulent flows arise from very complex fluid interactions, yet can be treated as diffusion-like processes in many instances. What cannot be done is to set universal constants in such models. Also, some flows cannot be accurately modeled using a diffusion formulation.

The rich multi-path scattering and diffraction in an urban environment does have some diffusion characteristics, and this is the reason the model fits the simulated data well in most cases. However, it is difficult to robustly relate city geometry metrics to the model parameters. Two courses of action exist for use of this model. One is a systematic study of simple geometries using ray tracing and analytic solutions (when possible) to understand where the model assumptions work and where they break down. Such studies can better define areas for model improvement and generalization. It might even be possible to set reasonable bounds on the few free parameters to enable generic characterization of city types. The other course is a more pragmatic, engineering approach and would use ray tracing methods to simulate cities of interest and provide the necessary parameters. A library of cities and their parameters would allow use of this simple functional form. This is analogous to the manner in which the Okamura-Hata model is used where one has a set of constants and functional forms depending on the setting, urban, dense urban, suburban, etc.

## VII. SUMMARY AND CONCLUSIONS

The stochastic urban model proposed in [4] has been critically inspected using simulated urban propagation results in four city environments. The functional form predicted by the model can be fit to most cities but it appears there are difficulties in robustly relating stochastic model parameters to city geometry parameters. The source of this difficulty is most likely due to the simple nature of diffusion processes compared to the complex workings of RF propagation.

The stochastic model does provide a more realistic functional behavior than other models (e.g. Okamura-Hata, Walfisch-Ikegami) which use power law expressions. The model may be improved upon by incorporating more of the propagation physics through a

systematic study. Also, the stochastic model can be utilized by building a library of stochastic model parameters for various city types.

## REFERENCES

- [1] Theodore Rappaport, "Wireless communications: Principles and Practice," *IEEE Trans. Antennas and Propagation*, Prentice Hall PTR, 2002.
- [2] Vinko Erceg, Saeed Ghassemzadeh, Maxwell Taylor, Dong Li and Donald Shilling, "Urban/suburban out-of-sight propagation modeling," *IEEE Communications Magazine*, Vol. 52, No. 5, pp. 56-61, June 1992.
- [3] Jerry Hampton, Naim Merheb, William Lain, Douglas Paunil, Robert Shuford and William Kasch, "Urban propagation measurements for ground based communications in the military UHF band," *IEEE Trans. Antennas and Propagation*, Vol. 54, No. 2, pp. 644-654, February 2006
- [4] Massimo Franceschetti, Joshua Bruck and Leonard J. Schulman, "A random walk model of wave propagation," *IEEE Trans. Antennas and Propagation*, Vol. 52, No. 5, pp. 1304-1317, May 2004
- [5] Massimo Franceschetti, "Stochastic Rays Pulse Propagation," *IEEE Trans. Antennas and Propagation*, Vol. 52, No. 10, pp. 2742-2752, October 2004.
- [6] K. J. Rizk, J. Wagner and F. Gardiol, "Two-dimensional ray-tracing modeling for propagation prediction in microcellular environments," *IEEE Trans. On Vehicular Tech.*, **46**, (2), pp.508-518, 1997.
- [7] H. Ling, R. C. Chou, S. W. Lee, "Shooting and Bouncing Rays: Calculating the RCS of an Arbitrarily Shaped Cavity," *IEEE Trans. Antennas and Propagation*, Vol. 37, No. 2, pp.1304-1317, Feb., 1989.